

ISSN: 0095-8972 (Print) 1029-0389 (Online) Journal homepage: <http://www.tandfonline.com/loi/gcoo20>


## Synthesis, molecular structure, and spectral analysis of copper(II) complexes derived from pyridinediols

Guillermo M. Chans, Elizabeth Gómez, Virginia Gómez-Vidales, R. Alfredo Toscano & Cecilio Álvarez-Toledano


To cite this article: Guillermo M. Chans, Elizabeth Gómez, Virginia Gómez-Vidales, R. Alfredo Toscano & Cecilio Álvarez-Toledano (2015) Synthesis, molecular structure, and spectral analysis of copper(II) complexes derived from pyridinediols, Journal of Coordination Chemistry, 68:2, 206-219, DOI: [10.1080/00958972.2014.982111](https://doi.org/10.1080/00958972.2014.982111)

To link to this article: <http://dx.doi.org/10.1080/00958972.2014.982111>

 View supplementary material 

 Accepted author version posted online: 29 Oct 2014.  
Published online: 21 Nov 2014.

 Submit your article to this journal 

 Article views: 163

 View related articles 

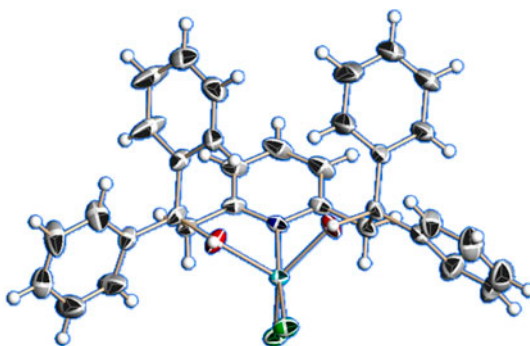
 View Crossmark data 

## Synthesis, molecular structure, and spectral analysis of copper (II) complexes derived from pyridinediols

GUILLERMO M. CHANS, ELIZABETH GÓMEZ\*, VIRGINIA GÓMEZ-VIDALES,  
R. ALFREDO TOSCANO and CECILIO ÁLVAREZ-TOLEDANO

Instituto de Química, Universidad Nacional Autónoma de México, México D.F., Mexico

(Received 1 July 2014; accepted 5 September 2014)



A series of mononuclear copper(II) complexes was synthesized by reaction of different 2,6-disubstituted pyridines with elemental Cu in a  $\text{CCl}_4/\text{DMSO}$  solvent system. Physical properties were analyzed using IR, optical spectroscopy, mass spectrometry, and EPR. Single-crystal X-ray diffraction for complexes **2a** and **4a** revealed that the molecular structure of **2a** is composed of a six-coordinate unit in which two ligands are linked to Cu(II) by oxygen and nitrogen donors. Conversely, in the molecular structure of **4a**, the Cu(II) has a slightly distorted trigonal bipyramidal arrangement, where the coordination environment around the copper ion is five-coordinate. EPR spectra of Cu(II) complexes were illustrated elaborately and some theoretical data were abstracted from EPR curves to support the proposed structures.

**Keywords:** Synthesis; Pyridinediols; Copper(II) complexes; Mononuclear; X-ray diffraction

### 1. Introduction

Lying on the edge between the d-block metals and the main group elements, copper is one of the most studied transition metals, owing to its electrical properties and commonness. The structure and bond properties of copper(II) compounds are of continuous interest in

\*Corresponding author. Email: [eligom@unam.mx](mailto:eligom@unam.mx)

inorganic chemistry [1, 2]. Recently, particular attention has been devoted to copper(II) complexes of multifunctional ligands [3–10]. The ligand multifunctionality attracts much attention owing to its chelating properties along with additional, not involved in the coordination, binding sites as potential linkers [11–14] and because of widespread applications in technology and crystal engineering [15]. Investigation of these complexes has become an interesting research field owing to relevance in bioinorganic and physical chemistry, in view of biological [3, 16–24], thermal [25, 26], and luminescent properties [27], with potential applications in materials. In addition, they have also been studied in the molecular magnetism area because they can act as building blocks for supramolecular architectures [28–31].

From the vast group of multidentate ligands, the so-called *O,N,O*-oxido pincer ligands [32–39] provide a scaffold to form Cu(II) complexes, which is interesting because the binding of this metal to O donors is likely to be weak; therefore, it is not surprising to find a relatively small number of complexes of late transition metals derived from oxido pincer ligands.

Copper complexes containing polypyridine ligands and their derivatives play a significant role as pharmacological agents, since they exhibit numerous biological activities such as antitumor [40], anticandida [41], antimicrobial [42], and antimicrobial activities [43, 44]. Pyridinediols are special cases of these metal receptors (figure 1). The combination of two hydroxy groups and the pyridine ring nitrogen donor makes these systems suitable for complexation of a variety of metals [45–52]. Moreover, the possibility of substituting the protons on the methylene carbon allows interesting electronic and steric variations to be introduced into ligands and their complexes. Such a study can give an insight into the influence of variable substitution to the geometry around Cu(II) or even to the packing of the molecule.

On the other hand, direct synthesis employing metal powders with organic ligands [53, 54] is also of interest in view of the fascinating complexes of unusual stoichiometry and structures that are formed in comparison with those obtained in conventional synthesis, which usually involves a metal salt as a starting material [34, 35, 55, 56]. It has been reported that copper metal is dissolved under extremely mild conditions by a solution of dimethylsulfoxide (DMSO) containing  $\text{CCl}_4$  to yield dimethyl sulfide and  $\text{CuCl}_2(\text{DMSO})_2$ , which reacts with the ligand [54]. This “one-step” synthesis of metal complexes starting from elemental metals is an active research field, which has undergone rapid progress [57–62]. These facts prompted us to explore the direct synthesis of complexes derived from pyridinediol and a zero-valent metal (Cu) as powder in a  $\text{CCl}_4/\text{DMSO}$  system, having in mind the advantages that direct synthesis allows, i.e. easier and extremely simple reaction conditions, some peculiar properties of the compounds obtained, and avoidance of impurities. Such advantages are particularly important with respect to this class of compounds, as reported in the literature, involving long and/or tedious preparation of the reagents and careful conditions [63–66].

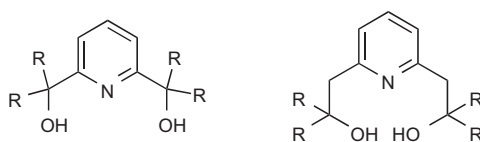


Figure 1. *O,N,O*-oxido pincer ligands.

Herein, we report the synthesis of two mononuclear copper(II) complexes coordinated by *O,N,O*-tridentate pyridyl alkoxy ligands, and their crystal structures by this straightforward and expeditious method, with the aim to evaluate the influence of the substituents and the chain length in the carbon  $\alpha$  to the pyridyl ring in complex formation.

## 2. Experimental

### 2.1. Materials and methods

All reagents, solvents, and **L1a** were obtained from commercial suppliers and used without purification. The reactions for ligand preparations were carried out under inert-gas conditions.

### 2.2. Preparation

**2.2.1. Synthesis of ligands.** *Synthesis of L1b,c:* These ligands were synthesized according to a modified literature procedure [46]. Thus, RLi 1 M (20.5 mM) was added dropwise to dimethyl pyridine-2,6-dicarboxylate (1.0 g, 5.1 mM) in THF (50 mL), at  $-78\text{ }^{\circ}\text{C}$ . After stirring at reflux for 6 h, the mixture was filtered through Celite under reduced pressure. Upon evaporation of the solvent and addition of water, the crude product was extracted with  $\text{CH}_2\text{Cl}_2$  (30 mL). The organic layer was evaporated, dried over  $\text{Na}_2\text{SO}_4$ , and purified by chromatography on silica gel using hexane/ethyl acetate (8 : 2) to give a white solid.

Ligands **L3a,b** were synthesized as described previously [67].

**2.2.2. Synthesis of complexes 2a–c and 4a,b.** Metal powder (1 mM), the corresponding ligand (1 or 2 mM), DMSO (0.5 mL), and  $\text{CCl}_4$  (3.5 mL) were placed in a flask and the mixture was heated, at  $65\text{ }^{\circ}\text{C}$  with magnetic stirring until total dissolution of the metal was observed (0.5–2 h). The reaction mixture was allowed to stand at room temperature, after which a precipitate was formed. The precipitate was filtered off and dried, at room temperature. Suitable single crystals of **2a** and **4a** were obtained by allowing them to stand in a hexane/methanol mixture.

**2.2.2.1. (L1a)<sub>2</sub>CuCl<sub>2</sub> (2a).** Green solid, m.p.  $168\text{--}169\text{ }^{\circ}\text{C}$  (dec.), ( $\text{C}_{14}\text{H}_{18}\text{Cl}_2\text{CuN}_2\text{O}_4$ ,  $M = 412.76\text{ g M}^{-1}$ ) 0.186 g, 0.450 mM (75% yield). IR (ATR)  $\nu$  3010, 2814, 2748, 2699, 2608, 1928, 1612, 1580, 1478, 1444, 1413, 1299, 1222, 1167, 1098, 1032, 957, 799, 695, 628, 530, 484 (Cu–O), 429, 376 (Cu–O), 315, 251 (Cu–N)  $\text{cm}^{-1}$ . FAB<sup>+</sup> MS  $m/z$  (rel. int., %) 342 (21, [(**L1a**)<sub>2</sub>Cu]<sup>+</sup>), 340 (40), 237 (12), 202 (52), 140 (100). UV–vis ( $\lambda_{\text{max}}$ , MeOH): 787 nm. HRMS (FAB<sup>+</sup>):  $m/z$  340.0484 calcd for  $\text{C}_{14}\text{H}_{18}\text{CuN}_2\text{O}_4$  [(**L1a**)<sub>2</sub>Cu]<sup>+</sup>; found 340.0487. Anal. Calcd for  $\text{C}_{14}\text{H}_{18}\text{Cl}_2\text{CuF}_4\text{N}_2\text{O}_4$ : C, 40.74; H, 4.40; N, 6.79. Found: C, 40.23; H, 4.74; N, 6.55.

**2.2.2.2. (L1b)<sub>2</sub>CuCl<sub>2</sub> (2b).** Green solid, m.p.  $185\text{ }^{\circ}\text{C}$  (dec.), ( $\text{C}_{22}\text{H}_{34}\text{Cl}_2\text{CuN}_2\text{O}_4$ ,  $M = 524.97\text{ g M}^{-1}$ ) 0.180 g, 0.343 mM (65% yield). IR (ATR)  $\nu$  3295, 3451, 3058, 2987, 2740, 2515, 1600, 1577, 1458, 1374, 1292, 1244, 1206, 1182, 1144, 1099, 1032, 954, 900,

845, 825, 768, 718, 695, 590, 475 (Cu–O), 449 (Cu–N), 398, 373 (Cu–O), 338, 315, 261 (Cu–N)  $\text{cm}^{-1}$ . FAB<sup>+</sup> MS  $m/z$  (rel. int., %) 454 (20, **(L1b)**<sub>2</sub>Cu<sup>+</sup>), 452 (39), 258 (26), 242 (12), 196 (100), 155 (22), 79 (26), 77 (10). UV–vis ( $\lambda_{\text{max}}$ , MeOH): 782 nm. HRMS calcd for C<sub>22</sub>H<sub>34</sub>CuN<sub>2</sub>O<sub>4</sub> [**(L1b)**<sub>2</sub>Cu–H]<sup>+</sup> 452.1736; found 452.1747. Anal. Calcd for C<sub>22</sub>H<sub>34</sub>Cl<sub>2</sub>CuN<sub>2</sub>O<sub>4</sub>·2C<sub>2</sub>H<sub>6</sub>OS: C, 45.84; H, 6.81; N, 4.11. Found: C, 46.06; H, 6.47; N, 4.76.

2.2.2.3. **(L1c)**<sub>2</sub>CuCl<sub>2</sub> (**2c**). Green solid, m.p. 190 °C (dec.), (C<sub>62</sub>H<sub>50</sub>Cl<sub>2</sub>CuN<sub>2</sub>O<sub>4</sub>,  $M = 1021.52 \text{ g M}^{-1}$ ) 0.067 g, 0.066 mM (29% yield). IR (ATR)  $\nu$  3289, 3083, 3054, 3024, 2918, 2801, 1729, 1652, 1569, 1489, 1439, 1405, 1364, 1316, 1256, 1206, 1169, 1092, 1049, 1023, 1002, 946, 906, 849, 832, 809, 769, 755, 734, 698, 634, 593, 496 (Cu–O), 383 (Cu–O), 333, 270 (Cu–N)  $\text{cm}^{-1}$ . FAB<sup>+</sup> MS  $m/z$  (rel. int., %) 949 (2, [**(L1c)**<sub>2</sub>Cu]<sup>+</sup>) 541 (39), 506 (9), 445 (100), 408 (100), 348 (34), 244 (25), 105 (53). UV–vis ( $\lambda_{\text{max}}$ , MeOH): 798 nm. HRMS (FAB<sup>+</sup>):  $m/z$  506.1181 calcd for C<sub>31</sub>H<sub>17</sub>CuNO<sub>2</sub> [**(L1c)**Cu]<sup>+</sup>; found 506.1182.

2.2.2.4. **L3a**CuCl<sub>2</sub> (**4a**). Green solid, m.p. 179–183 °C, (C<sub>33</sub>H<sub>29</sub>Cl<sub>2</sub>CuNO<sub>2</sub>,  $M = 606.04 \text{ g M}^{-1}$ ) 0.052 g, 0.086 mM (30% yield). IR (ATR)  $\nu$  3084, 3058, 3027, 2964, 2911, 1603, 1572, 1493, 1463, 1444, 1344, 1259, 1088, 1032, 1009, 945, 872, 799, 776, 739, 605, 551, 510 (Cu–O), 444 (Cu–N), 383 (Cu–O), 323, 285, 271 (Cu–N)  $\text{cm}^{-1}$ . FAB<sup>+</sup> MS  $m/z$  (rel. int., %) 569 (32, [**L3a**Cu–Cl]<sup>+</sup>), 534 (24, [**L3a**Cu–2 Cl]<sup>+</sup>), 472 (100), 436 (27), 376 (9), 531 (51), 271 (16), 183 (13), 105 (43), 77 (38). UV–vis ( $\lambda_{\text{max}}$ , MeOH) 816 nm. HRMS (FAB<sup>+</sup>):  $m/z$  569.1183; calcd for C<sub>33</sub>H<sub>29</sub>Cl<sub>2</sub>CuNO<sub>2</sub> [**L3a**Cu–Cl]<sup>+</sup>, found 569.1194. Anal. Calcd for C<sub>33</sub>H<sub>29</sub>Cl<sub>2</sub>CuF<sub>4</sub>NO<sub>2</sub>·2C<sub>2</sub>H<sub>6</sub>OS: C, 53.11; H, 5.42; N, 1.84. Found: C, 58.30; H, 5.25; N, 1.96.

2.2.2.5. **L3b**CuCl<sub>2</sub> (**4b**). Green solid, m.p. 150–155 °C, (C<sub>33</sub>H<sub>25</sub>Cl<sub>2</sub>CuF<sub>4</sub>NO<sub>2</sub>,  $M = 678.00 \text{ g M}^{-1}$ ) 0.460 g, 0.678 mM (48% yield). IR (ATR)  $\nu$  3256, 3060, 2994, 2912, 2685, 1639, 1602, 1505, 1463, 1406, 1312, 1224, 1162, 1113, 1060, 1015, 996, 942, 888, 836, 794, 744, 662, 630, 588, 562, 548, 510 (Cu–O), 432 (Cu–N), 409, 342 (Cu–O), 311, 294, 263 (Cu–N)  $\text{cm}^{-1}$ . FAB<sup>+</sup> MS  $m/z$  (rel. int., %) 606 (2, [**L3b**Cu–2 Cl]<sup>+</sup>), 544 (100), 430 (5), 219 (5). UV–vis ( $\lambda_{\text{max}}$ , MeOH): 820 nm. Anal. Calcd for C<sub>33</sub>H<sub>25</sub>Cl<sub>2</sub>CuF<sub>4</sub>NO<sub>2</sub>·1.5C<sub>2</sub>H<sub>6</sub>OS·2CH<sub>4</sub>O: C, 53.11; H, 4.93; N, 1.63. Found: C, 52.66; H, 4.70; N, 1.65.

### 2.3. Physical measurements

All compounds were characterized by IR spectra, recorded on a Bruker Tensor 27 spectrophotometer by ATR technique, and all data are expressed in wavenumbers ( $\text{cm}^{-1}$ ). UV–vis spectra were recorded in MeOH solution (0.8 g  $\text{mL}^{-1}$ ) in a 1-cm path length quartz cell on a Shimadzu U160 spectrophotometer. Melting points were obtained on a Melt-Temp II apparatus, and are uncorrected. The <sup>1</sup>H and <sup>13</sup>C NMR spectra were recorded on a Bruker Avance III, at 300 MHz (<sup>1</sup>H NMR) and 75 MHz (<sup>13</sup>C NMR) in chloroform-*d*. The MS-EI spectra were obtained by JEOL JMS-AX505 HA using 70 eV as ionization energy, and for MS-FAB, by JEOL JMS-SX102A using nitrobenzyl alcohol as matrix. EPR measurements were made in a quartz tube at 77 K with a Jeol JES-TE300 spectrometer operating at X-Band fashion at 100 kHz modulation frequency and a cylindrical cavity in mode TE<sub>011</sub>. The external calibration of the magnetic field was made with a precision Gauss meter Jeol

ES-FC5, and microwave frequency with a frequency counter 5350B HP. The spectrometer settings for all the spectra were as follows: center field, 300 mT; microwave power, 1 mW; microwave frequency, 9.10 GHz; sweep width,  $\pm 75.0$  mT; modulation width, 0.125 mT; time constant, 0.1 s; amplitude, 160; sweep time, 120 s; and accumulation, 1 scan. Spectral acquisition, manipulations, and simulation were performed using the program ES-IPRIT/TE, v1.916. The EPR spectrum was recorded as a first derivate, and the main parameter such as *g*-factor values were calculated according to Weil, Bolton, and Wertz [68]. All samples were measured in a DMSO/MeOH solution.

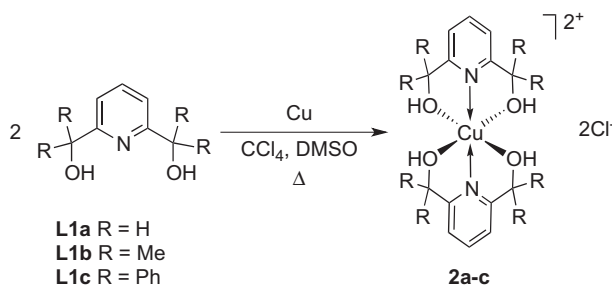
#### 2.4. Crystal structure determination

Single crystals of **2a** and **4a** suitable for X-ray diffraction studies were grown from its solution in a mixture of hexane:methanol or heptane:methanol (1 : 1 v/v). The crystals of each compound were mounted on a glass fiber at room temperature and then placed on a Bruker Smart Apex CCD diffractometer equipped with Mo K $\alpha$  radiation; decay was negligible in both cases. Details of crystallographic data collected on **2a** and **4a** are provided in table 1. Systematic absences and intensity statistics were used in space group determination. The structure was solved using direct methods [69].

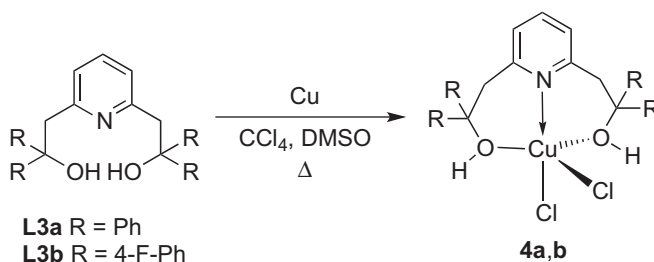
Anisotropic structure refinements were achieved using full matrix least-squares technique on all non-hydrogen atoms. All hydrogens were placed in idealized positions, based on hybridization, with isotropic thermal parameters fixed at 1.2 times the value of the attached atom. Structure solutions and refinements were performed using SHELXS-97 [70].

The interstitial solvent water molecule located in the channels of **2a** is disordered over a crystallographic twofold axis and was refined isotropically with partial fixed occupancy of 0.125. No hydrogens were located for this moiety.

For **4a**, both DMSO molecules display orientational disorder. In the first DMSO (O3 S1 C35 C36), the sulfur and the methyl groups show orientational disorder which was resolved over three orientations on approximately the same site and refined isotropically with 0.487, 0.295, and 0.217 occupancies, while the second DMSO (O4 S2 C37 C38) is disordered over two – almost equally populated 0.545(4)/0.455(4) – orientations and were refined anisotropically. The geometries of the PARTs were kept similar using the SAME restraint and displacement parameters in these disordered pieces were restrained using both SIMU and DELU.



Scheme 1. Syntheses of **2a-c**.

Scheme 2. Syntheses of **4a,b**.

### 3. Results and discussion

Pyridinediols **L1b–c** were synthesized by treating dimethyl 2,6-pyridinedicarboxylate with the appropriate Grignard reagent or alkyl lithium as described previously [46], followed by the reaction with elemental copper in  $\text{CCl}_4/\text{DMSO}$  [53] to afford the corresponding Cu complexes (scheme 1). Compounds **2a,b** have been described in the literature [34, 35, 55, 56]. Nevertheless, they were obtained by a different synthetic route using  $\text{Cu}(\text{NO}_3)_2 \cdot 3\text{H}_2\text{O}$  and  $\text{CuCl}_2 \cdot 2\text{H}_2\text{O}$  with 2 equivalents of the corresponding ligand.

Pyridinediols **L3a,b** were synthesized from lutidine and BuLi according to the literature procedure [67]. Ligands were obtained in good yields and characterized by spectroscopic methods. Complexes **4a,b** were obtained by reaction of **L3a,b** with elemental copper in equimolar quantities (scheme 2).

#### 3.1. Infrared spectral study

In table 2, Cu–N and Cu–O vibrations in the far-infrared area are shown. Based on data from earlier research [71, 72], we assign the bands at about  $445$  and  $260\text{ cm}^{-1}$  to the Cu–N vibration and the bands at approximately  $480$  and  $375\text{ cm}^{-1}$  to the Cu–O vibrations. The in-plane deformation of the uncoordinated pyridine ring in the ligands is observed at  $650\text{ cm}^{-1}$  [73]. Nevertheless, the *N*-coordination of the pyridine ring is confirmed in all complexes by the position of the absorption bands at  $700\text{ cm}^{-1}$ . Additionally, bands at  $429$ ,  $398$ , and  $409\text{ cm}^{-1}$  corresponding to out-of-plane deformation of the pyridine ring were assigned to **2a**, **2b**, and **4b**, respectively.

#### 3.2. Electronic absorption spectra

The UV–vis absorption spectra of **L1a–c**, **L3a,b**, and complexes **2a–c**, **4a**, and **4b** were recorded in MeOH. In the UV region, spectra of the five ligands display two bands from 200 to 240 nm (table 3). These bands are typical for pyridine ligands ( $\pi\text{--}\pi^*$  transitions) [74]. The visible spectra of the complexes reveal the presence of a broad absorption from 780 to 820 nm, which could be due to the d–d transition band of Cu(II) [75] with a low molar extinction coefficient value ( $\epsilon_{\text{max}}$   $33\text{--}36\text{ M}^{-1}\text{ cm}^{-1}$  for **2a–c** and  $97\text{--}113\text{ M}^{-1}\text{ cm}^{-1}$  for **4a, b**). The comparison of band shifts observed from 200 to 240 nm for complexes with their ligands indicates that the red shift is negligible.

Table 1. Crystal data and structure refinement for **2a** and **4a**.

	<b>2a</b>	<b>4a</b>
Formula weight	$C_{14}H_{18}CuN_2O_4Cl_2 \cdot 0.25 H_2O$	$C_{33}H_{29}Cl_2CuNO_2 \cdot 2 DMSO \cdot H_2O$
Temperature (K)	418.76	780.28
Wavelength (Å)	293(2)	298(2)
Unit cell dimensions	0.71073	0.71073
Crystal system, space group	Orthorhombic, <i>Cmca</i>	Monoclinic, <i>P 2<sub>1</sub>/c</i>
<i>a</i> (Å)	29.997(3)	17.384(2)
<i>b</i> (Å)	12.909(1)	11.408(1)
<i>c</i> (Å)	9.481(1)	19.968(2)
$\alpha$ (°)	90	90
$\beta$ (°)	90	104.921(2)
$\gamma$ (°)	90	90
<i>V</i> (Å <sup>3</sup> )	3671.2(7)	3826.3(6)
<i>D</i> <sub>calcd</sub> (Mg m <sup>-3</sup> )	1.515	1.354
<i>Z</i>	8	4
Absorption coefficient (mm <sup>-1</sup> )	1.501	0.861
<i>F</i> (0 0 0)	1720	1628
Crystal size (mm)	$0.52 \times 0.40 \times 0.18$	$0.414 \times 0.154 \times 0.084$
$\theta$ Range for data collection (°)	1.50–30.00	2.07–27.51
Limiting indices	$0 \leq h \leq 42, 0 \leq k \leq 18, 0 \leq l \leq 13$	$-22 \leq h \leq 22, -14 \leq k \leq 14, -25 \leq l \leq 17, -12 \leq k \leq 12, -16 \leq l \leq 16$
Reflections collected	5460	25,542
Independent reflections ( <i>R</i> <sub>int</sub> )	2730 (0.0574)	8763 (0.0971)
Completeness to $\theta = 30.00^\circ$	100.0%	99.9%
Absorption correction	None	Semi-empirical from equivalents
Maximum and minimum transmission		0.930 and 0.711
Refinement method	Full-matrix least-squares on <i>F</i> <sup>2</sup>	Full-matrix least-squares on <i>F</i> <sup>2</sup>
Data/restraints/parameters	2730/0/117	8763/140/504
Goodness-of-fit on <i>F</i> <sup>2</sup>	0.967	0.959
Final <i>R</i> indices [ <i>I</i> > 2 $\sigma$ ( <i>I</i> )]	<i>R</i> <sub>1</sub> = 0.0578, <i>wR</i> <sub>2</sub> = 0.1386	<i>R</i> <sub>1</sub> = 0.0652, <i>wR</i> <sub>2</sub> = 0.1304
<i>R</i> indices (all data)	<i>R</i> <sub>1</sub> = 0.1106, <i>wR</i> <sub>2</sub> = 0.1637	<i>R</i> <sub>1</sub> = 0.1667, <i>wR</i> <sub>2</sub> = 0.1673
Largest difference in peak and hole (e Å <sup>-3</sup> )	0.833 and -0.663	0.481 and -0.395



Table 2. Selected FT-IR spectral data ( $\text{cm}^{-1}$ ) for **2a–c** and **4a,b**.

Compound	Infrared data <sup>a</sup>		Py ring
	$\nu(\text{Cu-N})$	$\nu(\text{Cu-O})$	
<b>L1a</b>			658s
<b>L1b</b>			623br
<b>L1c</b>			655 m
<b>L3a</b>			654 m
<b>L3b</b>			664 m
<b>2a</b>	251s	484w, 376w	695br, 429 m
<b>2b</b>	449s, 261 m	475br, 373s	695s, 398 m
<b>2c</b>	270w	496 m, 383 m	698s
<b>4a</b>	444w, 271 m	510 m, 383br	698s
<b>4b</b>	432w, 263 m	510 m, 342w	695sh, 409w

<sup>a</sup>s, strong; m, medium; w, weak; sh, shoulder; br, broad.

Table 3. Characteristic bands ( $\lambda_{\text{max}}$ , in nm) and molar extinction coefficient ( $\epsilon$ ,  $\text{M}^{-1} \text{cm}^{-1}$ ) in UV-vis spectra (recorded in MeOH solution) for **2a–c** and **4a,b**.

Compound	$\lambda_{\text{max}}$ (nm) <sup>a</sup>	Molar extinction coefficient ( $\epsilon$ , $\text{M}^{-1} \text{cm}^{-1}$ )
<b>L1a</b>	208, 265	$6.6 \times 10^3$
<b>L1b</b>	207, 262	$9.3 \times 10^3$
<b>L1c</b>	208, 280	$5.0 \times 10^4$
<b>2a</b>	207, 264.0, 787br	36
<b>2b</b>	207, 262.0, 782br	36
<b>2c</b>	207, 266, 798br	33
<b>L3a</b>	209, 266	$4.4 \times 10^4$
<b>L3b</b>	208, 265	$4.1 \times 10^4$
<b>4a</b>	207, 269, 816br	113
<b>4b</b>	207, 266, 820br	97

<sup>a</sup>br, broad.

### 3.3. Mass spectra

Mass spectra of **2a–b** provide evidence for molecular formulas, owing to the loss of both chlorides: **2a**,  $\text{C}_{14}\text{H}_{18}\text{CuN}_2\text{O}_4$ ,  $M = 342 \text{ g M}^{-1}$ ; and **2b**,  $\text{C}_{22}\text{H}_{34}\text{CuN}_2\text{O}_4$  [ $(\text{L1b})_2\text{Cu-H}^+$ ],  $M = 452$ ; and whereas in **2c**, the loss of one ligand is also observed ( $\text{C}_{31}\text{H}_{17}\text{CuNO}_2$ , [ $(\text{L1c})\text{Cu}^+$ ],  $M = 506 \text{ g M}^{-1}$ ). On the other hand, the mass spectrum of **4a** ( $\text{C}_{33}\text{H}_{26}\text{Cl}_2\text{CuNO}_2$ ,  $M = 606 \text{ g M}^{-1}$ ) and **4b** ( $\text{C}_{33}\text{H}_{25}\text{Cl}_2\text{CuF}_4\text{NO}_2$ ,  $M = 678 \text{ g M}^{-1}$ ) did not show the molecular ion. Nevertheless, the loss of one ( $m/z$  534) and two ( $m/z$  569) chloride radicals is observed for **4a** and the loss of two chloride radicals ( $m/z$  606) for **4b**, confirming their formula weights.

### 3.4. EPR spectroscopy

Elongated and compressed Cu(II) octahedral complexes adopt different electronic ground states, since their unpaired electrons occupy the  $d_{x^2-y^2}$  or  $d_{z^2}$  atomic orbitals, respectively. These orbitals yield very different EPR spectra, whose lineshapes give evidence about the position of the singly occupied electron in either d-orbital. For a  $d_{x^2-y^2}$  complex, an axial symmetry pattern in the EPR spectrum is expected ( $g_{zz} \gg g_{yy} \approx g_{xx} > 2.0023$ ), whereas a  $d_{z^2}$  configuration yields an inverse axial symmetry ( $g_{yy} \approx g_{xx} \gg g_{zz} \approx 2.0023$ ) [76, 77].

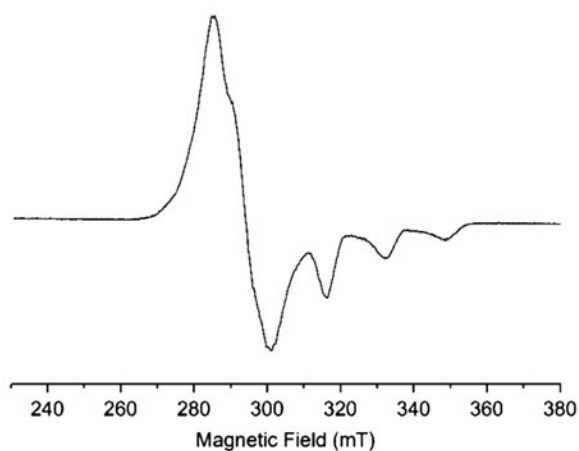


Figure 2. EPR spectrum (X band) of frozen solution of **2a** in DMSO at 77 K, showing an inverse axial symmetry.

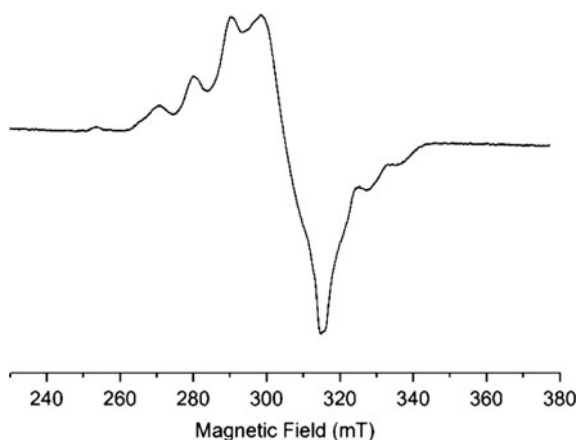


Figure 3. EPR spectrum of **4a** in frozen solution of DMSO.

Table 4. EPR data for **2<sup>a</sup>-c** and **4a,b**.<sup>a</sup>

Compound	$g_{zz}$	$g_{yy}$	$g_{xx}$	$g_{iso/ave}$	$A_{zz}$	$A_{yy}$	$A_{xx}$	Spectral symmetry	Molecular symmetry <sup>b</sup>
<b>2a</b>	2.01	2.21	2.21	2.14	154.3	8.0	8.0	Axial compressed	OC
<b>2b</b>	2.01	2.22	2.22	2.15	153.8	7.8	7.8	Axial compressed	OC
<b>2c</b>	2.34	2.07	2.07	2.16	147.5	8.2	8.2	Axial elongated	OE
<b>4a</b>	2.27	2.13	2.01	2.13	108.8	–	8.8	Rhombic	TBP
<b>4b</b>	2.30	2.12	2.01	2.14	110.3	–	7.8	Rhombic	TBP

<sup>a</sup>Constants ( $A$ ) are given in  $\text{cm}^{-1}$  and multiplied by a factor  $10^4$ .

<sup>b</sup>Symmetry assignment based on EPR spectroscopy, OC = octahedral compressed, OE = octahedral elongated, and TBP = trigonal bipyramidal.

The DMSO frozen glass (77 K) EPR spectra of the Cu(II) coordination compounds studied herein are shown in figures 2 and 3. EPR spectra display a signal in the center field, obtained for a system with  $S = 1/2$ , wherein the hyperfine lines correspond to copper

unpaired electron coupling with metal ion nuclei ( $I_{\text{Cu}} = 3/2$ ), characteristic of monomeric copper(II) complexes; no nitrogen hyperfine structure is observed, possibly because of the line broadening effects [78]. In particular, the EPR spectra obtained for **2a** and **2b** display an inverse axial symmetry with  $g_{yy} \approx g_{xx} \gg g_{zz} \approx 2.0023$  (figure 2) and show hyperfine coupling. The magnetic parameters obtained by simulation are listed in table 4, in agreement with a  $d_{z^2}$  ground state related to a compressed octahedral symmetry. Only a few structural studies with this geometry have been found in the literature [76, 79]. This structural feature had been also confirmed by the single-crystal structure analysis described below. On the contrary, **2c**, which has bulkier substituents ( $R = Ph$ ), imposes an octahedral distortion to the copper(II) complex, showing an ill-resolved axial spectra. The  $g$ -values ( $g_{zz} > g_{yy} \approx g_{xx} > 2.0023$ ) confirm that the unpaired electron on copper(II) corresponds to that geometry [80]. The  $g_{zz}$  and  $A_{zz}$  parameters ( $g_{zz} = 2.34$ ,  $A_{zz} = 147.5 \text{ cm}^{-1}$ ) show a slight decrease of  $g_{zz}$  and an increase of  $A_{zz}$  with respect to the elongated octahedral geometry ( $g_{zz} = 2.42$ ,  $A_{zz} = 124.0 \text{ cm}^{-1}$ ) [77, 81], indicating that the octahedron is slightly distorted towards square planar geometry. This behavior is due to variations in the orbital energy during the elongation.

The DMSO/MeOH frozen EPR spectra of **4a** and **4b** exhibit rhombic character as reflected by the  $g$  parameters, since  $g_{zz} > g_{yy} > g_{xx}$ , and show hyperfine coupling ( $I_{\text{Cu}} = 3/2$ ) (figure 3). The spectral patterns suggest a huge distortion of the copper site, as a pseudo-trigonal bipyramidal geometry [80, 82, 83]. This information is consistent with the crystal structure of **4a**.

### 3.5. Structural determination

Whereas Cu(II) environments have been well studied in unidentate or three bidentate ligands [18, 84], studies of symmetrical systems involving two tridentate ligands are relatively few [55, 56, 85]. The molecular structures of **2a** and **4a** were established by single-crystal X-ray diffraction analysis. ORTEP views of the complexes are shown in figure 4. In table 1 are gathered structural data; selected bond lengths and angles are given in table 5.

Compound **2a** was crystallized in the orthorhombic space group  $Cmca$  from hexane/methanol and consists of a crystal structure with a tridentate  $O,N,O$ -donor ligand and copper(II), in a discrete monomeric species. **2a** is isostructural and polymorphous to those structures obtained with  $\text{CuCl}_2$  and  $\text{Cu}(\text{NO}_3)_2$  [34, 35, 55]. Complex **2a** possesses a distorted compressed octahedral geometry, where Cu(II) is six-coordinate, surrounded by two nitrogens of the pyridyl groups and four oxygens of the alcohol arms. The Cu–N bond

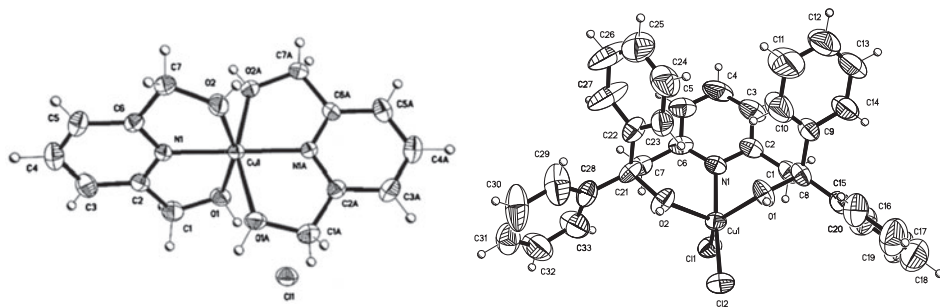


Figure 4. ORTEP view of **2a** and **4a**. Thermal ellipsoids at 30% probability.

Table 5. Selected bond lengths (Å) and angles (°) for **2a** and **4a**.

<b>2a</b>		<b>4a</b>	
Bond lengths		Bond lengths	
Cu(1)–O(1)	2.178(3)	Cu(1)–O(1)	2.167(3)
Cu(1)–O(2)	2.151(3)	Cu(1)–O(2)	2.144(3)
Cu(1)–N(1)	1.935(3)	Cu(1)–N(3)	1.998(3)
		Cu(1)–Cl(1)	2.261(1)
		Cu(1)–Cl(2)	2.215(1)
Bond angles		Bond angles	
O(2)–Cu(1)–O(1)	156.5(1)	O(2)–Cu(1)–O(1)	93.7(1)
O(2)–Cu(1)–N(1)	78.3(1)	O(2)–Cu(1)–N(1)	86.0(1)
O(2)–Cu(1)–O(2A)	94.2(2)	O(2)–Cu(1)–Cl(1)	124.4(1)
O(2)–Cu(1)–O(1A)	92.7(2)	O(2)–Cu(1)–Cl(2)	91.7(1)
O(2)–Cu(1)–N(1A)	101.3(1)	O(1)–Cu(1)–N(1)	81.0(1)
O(1)–Cu(1)–N(1)	78.3(1)	O(1)–Cu(1)–Cl(1)	140.7(1)
O(1)–Cu(1)–O(1A)	89.9(2)	O(1)–Cu(1)–Cl(2)	90.8(1)
O(1)–Cu(1)–N(1A)	102.2(1)	N(1)–Cu(1)–Cl(1)	91.5(1)
N(1)–Cu(1)–O(2A)	101.3(1)	N(1)–Cu(1)–Cl(2)	171.3(1)
N(1)–Cu(1)–N(1A)	179.4(2)	Cl(2)–Cu(1)–Cl(1)	96.7(1)

lengths in the apical positions (Cu(1)–N(1) = 1.935(3) Å) are shorter than the Cu–O bond lengths in the equatorial positions (Cu(1)–O(1) = 2.151(3), Cu(1)–O(2) = 2.178(3) Å), clearly indicating a Jahn–Teller compression [35]. A comparison between Cu(1)–O(2) bond lengths of **2a** with those described in the literature indicates that it is slightly shorter [34, 35, 55]. However, the remaining values of bond lengths and angles around the copper (II) in the complex do not show significant differences.

The OH groups are H-bonded to chlorides with H···Cl distances between 2.27 and 2.15 Å, bridging complex cations, showing a 2-D layer parallel to the (0 1 0) plane in the crystal packing, which is stabilized by weak hydrogen bonds (O1–H1···Cl1), as shown in the Supplemental Data. These H-bonds link neighboring Cu(II) monomers along the *b*-axis and their existence rationalizes the high thermodynamic stability of **2a**. The two pyridine rings are oriented almost perpendicular to each other, since the mean plane formed by pyridine ring atoms N(1)–C(2)–C(3)–C(4)–C(5) is 75.2 (0.1)°.

Compound **4a** crystallizes in the monoclinic system. The structure was solved in the  $P2_1/c$  space group. The coordination environment around copper is five-coordinate, consisting of one pyridyl nitrogen, two hydroxyl oxygens, and two chlorides. The molecular structure of **4a** has a distorted trigonal bipyramidal geometry, in which equatorial positions are occupied by Cl(1), O(1), and O(2) and the axial positions by the pyridyl N(1) and one chloride Cl(2). These results show opposite behavior to the preference of electronegative groups for the axial position on the TBP on similar silicon complexes [86–88].

Weak H-bonding interactions between the solvent and the complexes, or between the solvent molecules were determined. The shortest contacts are observed between the O(1)–H(1) proton of **4a** with the O(5) of water with an H···O distance of 1.95(4) Å [O···O 2.66(1) Å] and between the hydroxyl protons O(2)–H(2) of the complex with the DMSO oxygen O(3) (H···O 1.87(4) Å [O···O 2.63(1) Å]) (see the crystal packing in the Supplemental Data) [89].

A marked difference can be observed in the orientation of the chloride co-ligands. Thus, two chloride ligands complete a trigonal bipyramidal arrangement around copper (figure 4). The polyhedron is distorted, with the Cl–M–Cl angle of 96.7°. The apical positions (N–M–Cl) are separated by an angle of 171.3°.

The angular structural parameter  $\tau$  (index of trigonality) has been used for distinguishing between a trigonal bipyramidal (TBP) and square pyramidal (SP) geometry in five-coordinate complexes,  $\tau = (\beta - \alpha)/60^\circ$  where  $\alpha$  and  $\beta$  are the two largest angles [21, 90].  $\tau = 0$  for an ideal square pyramid ( $\alpha$  and  $\beta = 180^\circ$ ) and  $\tau = 1$  for an ideal trigonal bipyramid ( $\alpha = 120^\circ$  and  $\beta = 180^\circ$ ). Using this criterion, the  $\tau$  value is 0.51, indicating that the complex is distorted towards a trigonal bipyramidal geometry.

#### 4. Conclusion

The present study shows that the reaction of 2,6-*bis*-disubstituted pyridine derivatives with elemental copper produces monomeric compounds where one or two ligands are coordinated to copper. The magnetic behavior is fully in line with the assumption that the species **2a–c** exhibit a distorted octahedral geometry. Complexes **2a,b** show  $g_{yy} \approx g_{xx} \gg g_{zz} \approx 2.0023$ , consistent with a compressed symmetry, whereas **2c** displays  $g_{zz} > g_{yy} \approx g_{xx} > 2.0023$ , typical for an elongated symmetry. In the case of **4a–b**,  $g$  parameters suggest a pseudo-trigonal bipyramidal geometry. These geometries have been proved by single-crystal X-ray analysis.

The preference for formation of six-coordinate **2a–c** could be associated to the formation of two five-membered rings from the pyridine ligands that stabilize a cationic complex. However, in the case of **4a,b**, they are formed through the complexation of the pyridine ligands with the elemental copper. The formation of these five-coordinate complexes seems to be highly favored owing to the six-membered rings, which are probably stabilized due to increasing steric factor on the pyridine carbons.

#### Supplementary material

CCDC-1001885 (**2a**) and CCDC-1001886 (**4a**) contain the supplemental crystallographic data for this paper. These data can be obtained free of charge from the Cambridge Crystallographic Data Center via [www.ccdc.ac.uk/data\\_request/cif](http://www.ccdc.ac.uk/data_request/cif).

#### Acknowledgements

We gratefully acknowledge financial support from Instituto de Química, UNAM. One of the authors, G.M.C., is thankful to The World Academy of Sciences (TWAS) and the Consejo Nacional de Ciencia y Tecnología (CONACYT) for awarding a post-doctoral research fellowship. We also appreciate the technical assistance of Rocío Patiño, María de la Paz Orta Pérez, Alejandra Núñez Pineda, Luis Velasco, and Javier Pérez.

#### Supplemental data

Supplemental data for this article can be accessed here [<http://dx.doi.org/10.1080/00958972.2014.982111>].

## References

- [1] B.P. Murphy. *Coord. Chem. Rev.*, **124**, 63 (1993).
- [2] B.J. Hathaway, In *Comprehensive Coordination Chemistry: The Synthesis, Reactions, Properties, and Applications of Coordination Compounds*, G. Wilkinson, R.D. Gillard, J.A. McCleverty (Eds), Pergamon Press, Oxford (1987).
- [3] L.-D. Wang, K. Zheng, Y.-T. Li, Z.-Y. Wu, C.-W. Yan. *J. Mol. Struct.*, **1037**, 15 (2013).
- [4] G. Psomas, A. Tarushi, E.K. Efthimiadou, Y. Sanakis, C.P. Raptopoulou, N. Katsaros. *J. Inorg. Biochem.*, **100**, 1764 (2006).
- [5] Z. Zude, Z. Tao, X. Xingyou, C. Hua, L. Qingliang. *J. Coord. Chem.*, **48**, 265 (1999).
- [6] D.J. Hutchinson, L.R. Hanton, S.C. Moratti. *Inorg. Chem.*, **49**, 5923 (2010).
- [7] F. Yu. *Cryst. Struct. Commun.*, **67**, m331 (2011).
- [8] J. Ran, X. Li, Q. Zhao, Z. Qu, H. Li, Y. Shi, G. Chen. *Inorg. Chem. Commun.*, **13**, 526 (2010).
- [9] L.-L. Zheng, W.-X. Zhang, L.-J. Qin, J.-D. Leng, J.-X. Lu, M.-L. Tong. *Inorg. Chem.*, **46**, 9548 (2007).
- [10] A.W. Hanson. *Cryst. Struct. Commun.*, **42**, 501 (1986).
- [11] D.W. Min, S.S. Yoon, D.Y. Jung, C.Y. Lee, Y. Kim, W.S. Han, S.W. Lee. *Inorg. Chim. Acta*, **324**, 293 (2001).
- [12] B.O. Patrick, C.L. Stevens, A. Storr, R.C. Thompson. *Polyhedron*, **22**, 3025 (2003).
- [13] S. Noro, S. Kitagawa, T. Wada. *Inorg. Chim. Acta*, **358**, 423 (2005).
- [14] L. Xue, F. Luo, Y.-X. Che, J.-M. Zheng. *J. Mol. Struct.*, **832**, 132 (2007).
- [15] S. Fukuzumi, H. Kotani, H.R. Lucas, K. Doi, T. Suenobu, R.L. Peterson, K.D. Karlin. *J. Am. Chem. Soc.*, **132**, 6874 (2010).
- [16] J.J. Martínez Medina, M.S. Islas, L.L. López Tévés, E.G. Ferrer, N.B. Okulik, P.A.M. Williams. *J. Mol. Struct.*, **1058**, 298 (2014).
- [17] P.S. Lopes, D.A. Paixão, F.C.S. de Paula, A.M.D.C. Ferreira, J. Ellena, S. Guilardi, E.C. Pereira-Maia, W. Guerra. *J. Mol. Struct.*, **1034**, 84 (2013).
- [18] B. Kupcewicz, M. Ciolkowski, B.T. Karwowski, M. Rozalski, U. Krajewska, I.-P. Lorenz, P. Mayer, E. Budzisz. *J. Mol. Struct.*, **1052**, 32 (2013).
- [19] S. Sarkar, T. Mukherjee, S. Sen, E. Zangrando, P. Chattopadhyay. *J. Mol. Struct.*, **980**, 117 (2010).
- [20] S.O. Bahaffi, A.A. Abdel Aziz, M.M. El-Naggar. *J. Mol. Struct.*, **1020**, 188 (2012).
- [21] M. Choudhary, R.N. Patel, S.P. Rawat. *J. Mol. Struct.*, **1060**, 197 (2014).
- [22] A.L. Abuhijleh. *J. Mol. Struct.*, **980**, 201 (2010).
- [23] I. Ali, W.A. Wani, K. Saleem, M.-F. Hsieh. *J. Coord. Chem.*, **67**, 2110 (2014).
- [24] M. Kose, M. Digrak, I. Gonul, V. McKee. *J. Coord. Chem.*, **67**, 1746 (2014).
- [25] A. Trzesowska-Kruszyska. *J. Mol. Struct.*, **1017**, 72 (2012).
- [26] A. Beheshti, V. Nobakht, L. Carlucci, D.M. Proserpio, C. Abrahams. *J. Mol. Struct.*, **1037**, 236 (2013).
- [27] S. Mandal, R. Modak, S. Goswami. *J. Mol. Struct.*, **1037**, 352 (2013).
- [28] M. Outirite, B. Mernari, F. Bentiss, F. Capet, M. Lagrenée. *J. Mol. Struct.*, **989**, 60 (2011).
- [29] I.F. Santos, G.P. Guedes, L.A. Mercante, A.M.R. Bernardino, M.G.F. Vaz. *J. Mol. Struct.*, **1011**, 99 (2012).
- [30] B.L. Solomon, C.P. Landee, M.M. Turnbull, J.L. Wikaira. *J. Coord. Chem.*, (2014). doi: .
- [31] Y. Wu, Y. Mu, L. Bai, S. Guo, J. Zhao, D.-S. Li. *J. Coord. Chem.*, **67**, 1629 (2014).
- [32] A.M.S. Silva, L.M.P.M. Almeida, J.S. Cavaleiro, C. Foces-Foces, A.L. Llamas-Saiz, C. Fontenas, N. Jagerovic, J. Elguero. *Tetrahedron*, **53**, 11645 (1997).
- [33] W.-J. Gu, B.-X. Wang. *Acta Crystallogr. Sect. E*, **65**, o233 (2009).
- [34] G.C. Vlahopoulou, D.I. Alexandropoulos, C.P. Raptopoulou, S.P. Perlepes, A. Escuer, T.C. Stamatatos. *Polyhedron*, **28**, 3235 (2009).
- [35] S. Winter, W. Seichter, E. Weber. *Z. Anorg. Allg. Chem.*, **630**, 434 (2004).
- [36] R. Vafazadeh, R. Esteghamat-Panah, A.C. Willis, A.F. Hill. *Polyhedron*, **48**, 51 (2012).
- [37] R.N. Patel, V.L.N. Gundla, D.K. Patel. *Polyhedron*, **27**, 1054 (2008).
- [38] R.N. Patel, N. Singh, V.L.N. Gundla. *Polyhedron*, **25**, 3312 (2006).
- [39] A. Klein, K. Butsch, J. Neudörfl. *Inorg. Chim. Acta*, **363**, 3282 (2010).
- [40] J.D. Ranford, P.J. Sadler, D.A. Tocher. *J. Chem. Soc., Dalton Trans.*, 3393 (1993).
- [41] M. Geraghty, V. Sheridan, M. McCann, M. Devereux, V. McKee. *Polyhedron*, **18**, 2931 (1999).
- [42] D.K. Saha, U. Sandbhor, K. Shirisha, S. Padhye, D. Deobagkar, C.E. Anson, A.K. Powell. *Bioorg. Med. Chem. Lett.*, **14**, 3027 (2004).
- [43] M.A. Zoroddu, S. Zanetti, R. Pogni, R. Basosi. *J. Inorg. Biochem.*, **63**, 291 (1996).
- [44] R.N. Patel, N. Singh, K.K. Shukla, V.L.N. Gundla, U.K. Chauhan. *Spectrochim. Acta, Part A*, **63**, 21 (2006).
- [45] E. Gómez, Z. Hernández, C. Alvarez-Toledano, R.A. Toscano, V. Santes, P. Sharma. *J. Organomet. Chem.*, **648**, 280 (2002).
- [46] E. Gómez, V. Santes, V. de la Luz, N. Farfán. *J. Organomet. Chem.*, **622**, 54 (2001).
- [47] B. Kaptein, G. Barf, R.M. Kellogg, F. Van Bolhuis. *J. Org. Chem.*, **55**, 1890 (1990).
- [48] H. Mack, M.S. Eisen. *J. Chem. Soc., Dalton Trans.*, 917 (1998).
- [49] J.J.H. Edema, R. Libbers, A.M. Ridder, R.M. Kellogg, F. van Bolhuis, H. Kooijman, A.L. Spek. *J. Chem. Soc., Chem. Commun.*, 625 (1993).

- [50] J.M. Berg, R.H. Holm. *J. Am. Chem. Soc.*, **106**, 3035 (1984).
- [51] T.K. Prakasha, A. Chandrasekaran, R.O. Day, R.R. Holmes. *Inorg. Chem.*, **35**, 4342 (1996).
- [52] J.M. Berg, R.H. Holm. *J. Am. Chem. Soc.*, **107**, 917 (1985).
- [53] R. Gutiérrez, J. Vázquez, R.A. Vázquez, Y. Reyes, R.A. Toscano, M. Martinez, C. Álvarez. *J. Coord. Chem.*, **54**, 313 (2001).
- [54] Y. Tezuka, M. Miya, A. Hashimoto, K. Imai. *J. Chem. Soc., Chem. Commun.*, 1642 (1987).
- [55] A. Klein, K. Butsch, S. Elmas, C. Biewer, D. Heift, S. Nitsche, I. Schlipf, H. Bertagnolli. *Polyhedron*, **31**, 649 (2012).
- [56] A. Klein, S. Elmas, K. Butsch. *Eur. J. Inorg. Chem.*, **2009**, 2271 (2009).
- [57] D.G. Alexander, B.I. Kharisov, G. Gojon-Zorrilla, D.A. Garmovskii. *Russ. Chem. Rev.*, **64**, 201 (1995).
- [58] S.R. Petrusenko, V.N. Kokozay, O. Yu Vassilyeva, B.W. Skelton. *J. Chem. Soc., Dalton Trans.*, 1793 (1997).
- [59] V.N. Kokozay, A.V. Sienkiewicz. *Polyhedron*, **14**, 1547 (1995).
- [60] V.V. Skopenko, V.N. Kokozay, V.R. Polyakov, A.V. Sienkiewicz. *Polyhedron*, **13**, 15 (1994).
- [61] V. Kokozay, A. Sienkiewicz. *Polyhedron*, **12**, 2421 (1993).
- [62] G. Nifontova, I. Lavrentiev. *Transition Met. Chem.*, **18**, 27 (1993).
- [63] E. Boschmann, L.M. Weinstock, M. Carmack. *Inorg. Chem.*, **13**, 1297 (1974).
- [64] J.T. Wroblewski, G.J. Long. *Inorg. Chim. Acta*, **30**, 221 (1978).
- [65] S.F. Mason, R.D. Peacock. *J. Chem. Soc., Dalton Trans.*, 226 (1973).
- [66] S.N. Choi, R.D. Bereman, J.R. Wasson. *J. Inorg. Nucl. Chem.*, **37**, 2087 (1975).
- [67] B. Koning, J. Buter, R. Hulst, R. Stroetinga, R.M. Kellogg. *Eur. J. Org. Chem.*, **2000**, 2735 (2000).
- [68] J.A. Weil, J.R. Bolton, J.E. Wertz, Electron Spin Resonance. Elementary Theory Practical Applications, p. 568, Wiley, New York, NY (1994).
- [69] A. Altomare, G. Cascarano, C. Giacovazzo, A. Guagliardi, M.C. Burla, G. Polidori, M. Camalli. *J. Appl. Crystallogr.*, **27**, 435 (1994).
- [70] G. Sheldrick. *Acta Crystallogr., Sect. A*, **64**, 112 (2008).
- [71] G.A. Van Albada, M.T. Lakin, N. Veldman, A.L. Spek, J. Reedijk. *Inorg. Chem.*, **34**, 4910 (1995).
- [72] G.A. van Albada, W.J.J. Smeets, A.L. Spek, J. Reedijk. *Inorg. Chim. Acta*, **260**, 151 (1997).
- [73] K. Nakamoto. In *Part B Infrared and Raman Spectra of Inorganic and Coordination Compounds*, 5th Edn, Wiley, New York, NY (1997).
- [74] K.R. Kyle, C.K. Ryu, P.C. Ford, J.A. DiBenedetto. *J. Am. Chem. Soc.*, **113**, 2954 (1991).
- [75] Z. Wei, X. Xie, J. Zhao, L. Huang, X. Liu. *Inorg. Chim. Acta*, **387**, 277 (2012).
- [76] J.M. Holland, X. Liu, J.P. Zhao, F.E. Mabbs, C.A. Kilner, M. Thornton-Pett, M.A. Halcrow. *J. Chem. Soc., Dalton Trans.*, 3316 (2000).
- [77] S.K. Hoffmann, J. Goslar, S. Lijewski, K. Basiński, A. Gąsowska, L. Łomozik. *J. Inorg. Biochem.*, **111**, 18 (2012).
- [78] Y. Nonaka, T. Tokii, S. Kida. *Bull. Chem. Soc. Jpn.*, **47**, 312 (1974).
- [79] B. Kozlevčar, A. Golobič, P. Strauch. *Polyhedron*, **25**, 2824 (2006).
- [80] D. Kroczevska, K. Bogusz, B. Kurzak, J. Jezierska. *Polyhedron*, **21**, 295 (2002).
- [81] G. Tabbi, A. Giuffrida, R.P. Bonomo. *J. Inorg. Biochem.*, **128**, 137 (2013).
- [82] B. Kurzak, A. Kamecka, K. Bogusz, J. Jezierska. *Polyhedron*, **26**, 4345 (2007).
- [83] D. Kroczevska, B. Kurzak, J. Jezierska. *Polyhedron*, **25**, 678 (2006).
- [84] M. Sarma, B. Mondal. *Dalton Trans.*, **41**, 2927 (2012).
- [85] J. Pinart, C. Petitfaux, J. Faucherre. *Bull. Soc. Chim. Fr.*, 4534 (1972).
- [86] A. Chandrasekaran, R.O. Day, R.R. Holmes. *Organometallics*, **17**, 5114 (1998).
- [87] A. Chandrasekaran, R.O. Day, R.R. Holmes. *Organometallics*, **15**, 3182 (1996).
- [88] C. Breliere, F. Carre, R.J.P. Corriu, M. Poirier, G. Royo. *Organometallics*, **5**, 388 (1986).
- [89] T. Steiner. *Angew. Chem. Int. Ed.*, **41**, 48 (2002).
- [90] A.W. Addison, T.N. Rao, J. Reedijk, J. van Rijn, G.C. Verschoor. *J. Chem. Soc., Dalton Trans.*, 1349 (1984).